Test Method to Quantify the Wicking Properties of Insulation Materials Designed to Prevent Interstitial Condensation

Andrea Binder **Daniel Zirkelbach** **Hartwig Künzel, PhD**
Member ASHRAE

ABSTRACT

Applying insulation to the interior side of the wall often is the only option for a thermal retrofit, especially when heritage buildings are concerned. In order to avoid harmful condensation beneath the interior insulation, most systems include a vapor retarding layer which also reduces the drying potential of the wall. Therefore, vapor-permeable insulation materials have been developed that are capable of wicking condensing moisture away from the wall/insulation interface back to the surface in contact with the indoor air. A widely used and extensively studied material with such characteristics is Calcium-silicate. Following an increasing demand, several water-wicking insulation materials have appeared on the market. However, there is no consensus yet on how to quantify their efficiency in preventing critical moisture conditions at the interface.

Since the water absorption coefficient of a porous material is dominated by the largest capillaries, this coefficient does not seem appropriate for the characterization of the material's liquid transport properties in the hygroscopic region. Therefore, a new measuring method for wicking insulation materials has been devised. One side of a laterally sealed material sample is controlled at a temperature below the dew-point by a Peltier-unit, while the other side is exposed to the air of a climate chamber. At the dynamic equilibrium of the opposing moisture fluxes (liquid and vapor), moisture distribution recordings are performed using Nuclear magnetic resonance (NMR). This allows the determination of the material's liquid diffusivity function in the hygroscopic region, whose magnitude is a measure for the wicking efficiency of the material.

INTRODUCTION

Rising oil prices and new energy regulations call for thermal retrofits of existing buildings, including those belonging to the national heritage. The majority of such buildings in Europe are built in a massive way (brick or natural stone), and many have stucco façades. Due to preservation provisions, the original façade has to be maintained. In these cases, the only option to improve the thermal performance of the wall is interior insulation. By applying an insulation layer to the interior side of a wall, its temperature is reduced. The possibility of damage to sensitive structures caused either by condensation of indoor humidity (Figure 1, left) or by driving rain impact is often posed in this context. While a vapor retarder (Figure 1, middle) can prevent condensation, it also reduces the drying of moisture towards the interior. The fact that this may lead to critical humidity conditions in walls affected by wind-driven rain or rising damp has provoked reservations against vapor retarders among preservationists in Europe.

Manufactures have reacted quickly by developing vapor permeable insulation materials that do not need a vapor retarder as they are able to wick any condensation from the original wall structure (Figure 1, right). For this purpose, holohedral agglutination of insulation and wall has to be secured. In the meantime, several wicking insulation materials (e.g. Calcium-silicate, Autoclave Aerated Concrete-based mineral foam, hydrophilic glass fiber, cellulose fiber) are available, all of them claiming to prevent interstitial condensation. However, up to now there is no reliable way to quantify the wicking properties of these materials under the conditions they face after installation. This paper describes the development of a testing

A. Binder *is a researcher,* ***D. Zirkelbach*** *is deputy head, and* ***H.M. Künzel*** *is head of the department of Hygrothermics at Fraunhofer—Institute for Building Physics in Holzkirchen, Germany.*

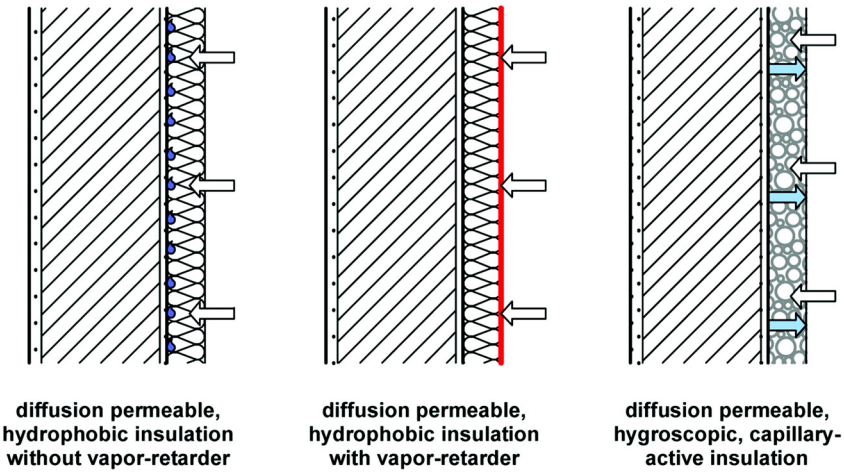

Figure 1 *Different systems used to interiorly insulate massive walls.*

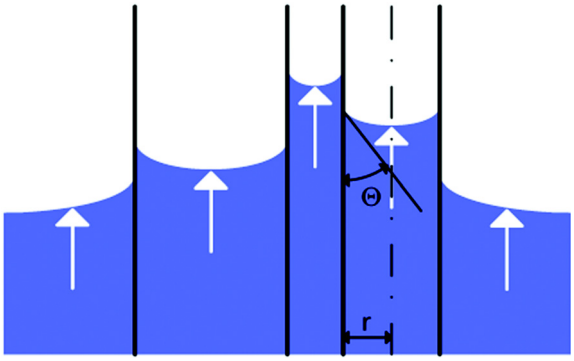

Figure 2 *Capillary ascension in ideal material pores due to capillary pressure.*

device to determine the hygrothermal behavior and liquid transport ability of different insulation materials in the hygroscopic moisture range under non-isothermal conditions. The results are employed to fine-tune the liquid transport properties via hygrothermal simulation.

Principles of Moisture Storage and Transport in Hydrophilic Porous Media

Moisture in a hydrophilic porous material can be present as vapor or liquid. Impartial of its aggregate state inside the material, the transfer of this moisture is carried out in two basic ways: Either through vapor diffusion into the material—the driving force here is a gradient of partial pressure; or through the suction of liquid water—responsible here is a gradient of relative humidity or the capillary suction power of material pores. With rising relative humidity inside the material pores, more and more moisture is stored at the inner surface of the pores (surface diffusion). Dependent on the pore size, the filling degree can reach from a mono-molecular or multi-molecular moisture film up to a complete fill. As most materials show a wide range of pore sizes, the filling degree inside the pores can be different at the same time. With rising liquid moisture inside the pores, an increasing liquid moisture transport begins along the gradient of relative humidity. When the pores are completely filled, another driving force sets in: capillary suction pressure (Figure 2). Due to the existing suction pressure, the transport velocity here can exceed that inside the surface moisture film many times. The pressure thereby is the higher, the smaller the pore radius is. The fluid therefore rises highest in small pores. With rising pore size, the suction pressure drops, while the suction speed increases. These fluid moisture transport phenomena are called capillary activity.

Dependent on boundary conditions, the impact on building materials and moisture transport phenomena inside its

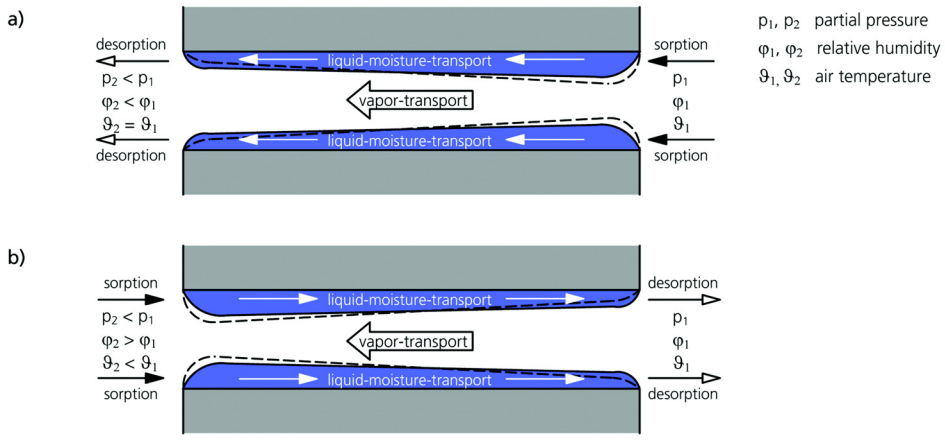

Figure 3 *Moisture transport phenomena in pores of hydrophilic media under (a) isothermal and (b) non-isothermal boundary conditions.*

pores are different. Basically, two different boundary conditions have to be distinguished: isothermal (Figure 3a) and non-isothermal conditions (Figure 3b). Isothermal conditions with liquid moisture as well as vapour transport going into the same direction usually exist in summer. Non-isothermal conditions, however, apply during winter and are of particular importance with regard to interior insulation. Due to the existing gradient of partial pressure, vapor diffusion from the interior to the cold side of the wall begins. Opposing is a gradient of relative humidity; the liquid transport therefore proceeds from the outside back to the interior. The interacting, opposing moisture fluxes may lead to a dynamic equilibrium in time.

While there are equations to describe moisture transport phenomena such as vapour diffusion, suction pressure and velocity in ideal pores as shown in Figures 2 and 3, their characterization inside a building material is much more complex, due to its varied pore structure and interacting moisture transport processes. Therefore, a complete numerical calculation is still not possible.

Conventional Test Procedures and their Limitations

Transient hygrothermal computational simulations have proved to show good performance in many applications in practice. To produce acceptable correlations between calculated and measured moisture behavior, exact determination of the material properties is essential. For most hygrothermal material properties, standardized or approved testing methods are available (DIN EN ISO 12571; DIN EN ISO 12572; DIN EN ISO 15148). The determination of liquid transport, however, can be approached in different manners. There is growing evidence that the existing methods may not be sufficiently accurate for characterizing the moisture behavior of interior insulation materials. To determine a material's liquid transport, test procedures usually involve wetting of either a surface or the complete material. Information about liquid transport coefficients is then gained from the observed moisture absorption or redistribution by periodical scanning of the material samples (Krus 1995). Other test methods include drying the wet material under controlled boundary conditions (Scheffler and Plagge 2009; Holm and Krus 1998). As all test methods mentioned are not yet standardized, no such characteristics are available for many building materials. Therefore, a simplified method to generate the liquid transport characteristics out of other hygrothermal material properties has been devised (Krus et al. 1997; Künzel 1994). This test method, however, has been developed only to allow an estimation of the liquid transport, when no specific liquid transport properties are at hand, and should therefore be used with care.

There are certain limitations and problems with the application of the liquid transport properties determined by conventional test methods in the special case of interior insulation materials. It has been assumed so far that liquid transport properties identified for high moisture contents (occurring in materials exposed to wind-driven rain) can be transferred to lower moisture levels and different modes of wetting. Additionally, all tests are executed in isothermal conditions. As liquid, as well as vapor transport, have the same direction, a distinction between the two cannot be made. No information can be gained therefore about the quantity of each transport mode by itself. As described before, the relevant boundary conditions that apply to interior insulation materials are non-isothermal. The moisture content inside the material pores accumulates due to a gradient of partial pressure and vapor diffusion from the interior. With rising moisture content, an increasing capillary transport from the exterior side of the material back to the surface in contact with indoor air sets in. These interactions are not represented by conventional test methods. Additionally, the high amounts of water applied in the conventional tests

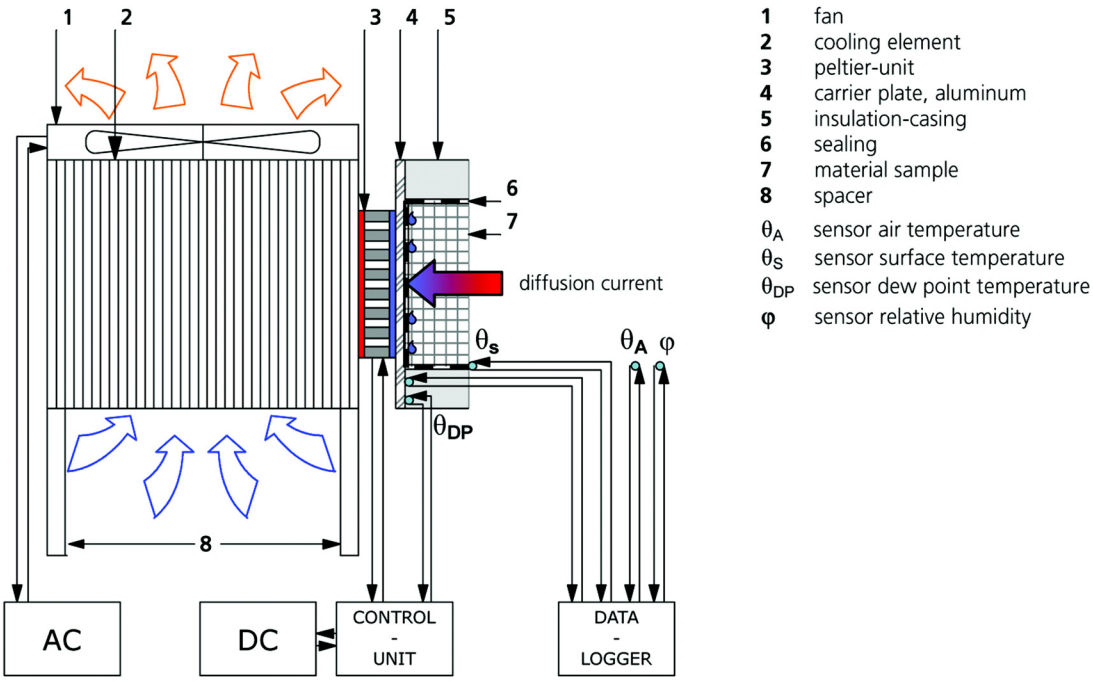

Figure 4 *Schematic setup for the Interstitial Condensation Tests.*

might be inappropriate for some materials, as it may lead to changes in the material structure, e.g. swelling or agglutinating of fibrous materials. Therefore, it seems wise to measure the capillary activity of an interior insulation material under the conditions it has to face in real-life application.

PROPOSAL OF A NON-ISOTHERMAL TEST SETUP: INTERSTITIAL CONDENSATION TEST

To determine the capillary activity of materials used as interior insulation, a new test setup has been developed. In imitation of real-life boundary conditions, the wicking properties are derived by tests without the application of liquid water and under non-isothermal conditions. In this way, significant characteristics can be identified for the specific conditions of interior insulation. The test setup is shown in Figure 4. Under laboratory conditions, a dew-point undercut is applied to one side of a laterally sealed material sample. This produces a gradient of temperature and partial pressure, and consequently vapor diffusion into the material. The adsorbed moisture is condensing at the sealed back side of the material, where it causes an increase of relative humidity; hence, the moisture content inside the material sample is rising. Due to the increasing gradient of relative humidity, a liquid transport back to the front of the material sets in. Eventually, the opposing moisture fluxes will reach a dynamic equilibrium. To reveal the hygrothermal behavior of the material samples during testing, two modes of measuring are taken. Through periodic gravimetrical measurements, the moisture gain is analyzed and documented for the test period. The moisture distribution in the material cross-section is measured periodically by using nuclear magnetic resonance spectroscopy (NMR).

Test Equipment

To produce a temperature at the back side of the material sample that falls below the dew point, thermo-electrical devices called “Peltier-unit” (PU) are used. Based on a thermoelectric effect called the Peltier-effect, one side of the element is cooled down, while the other side is heated. As a strong dependency exists between the hot and cool sides of the PU, the emerging heat has to be conducted away from the element in order to gain acceptable performance. The units used in the experiments are single-level units with a maximum temperature gradient of 73.0 K. They possess a waterproof coating to avoid possible malfunctions resulting from moisture condensing during testing. The PUs are applied to a passive cooling element to provide for sufficient cooling. To enhance the circulation around the cooling element further, the whole element is put onto spacers; additionally, a high capacity fan is installed on top of the cooling element. An aluminum carrier plate is connected to the cold side of the PU. The connection between all elements has to be flawless in order to provide good heat transfer, heat conductive paste therefore is applied. A temperature sensor (PT 100) at the

front of the carrier plate forms an interface with the control unit. This control unit regulates the power supply and therefore, the cooling power of the PU. To regulate and document the boundary conditions as well as the thermal behavior of the tested material samples, temperature and humidity sensors are installed. A conventional laboratory balance is used to measure and document the water content inside the material. The moisture distribution analysis is done by using nuclear magnetic resonance (NMR) spectroscopy.

Materials Tested

The material most commonly mentioned in connection with capillary activity and wicking ability is calcium-silicate (CS). One of the products examined in this paper therefore is a board-shaped hydrophilic CS material made out of the two components sand and lime, with a very fine and open-pored structure. It is used for interior insulation, mold prevention, and collateral drying of moist masonry. Another mineral insulation board used for testing is an Autoclaved Aerated Concrete Foam (AACF); natural protein used as air-entraining agent. While its pore structure is not as fine as that of CS, its porosity is slightly higher. The common usage is the interior insulation of walls and exterior ceilings. Both materials described above are porous and hydrophilic. Therefore, they are considered to be somewhat capillary active. As a contrast, a material has been tested that is porous, but hydrophobic. The mineral wool (MW) used in the tests is usually used for external thermal insulation composite systems (ETICS).

Preparation of Material Samples

The experiments should provide significant results, preferably in a short time. As with rising thickness of insulation samples, the time span to the achievement of a dynamic equilibrium between the moisture fluxes increases, material samples for the tests have to be of adequate thickness. The maximum width of 50.0 millimeters (mm) is constrained by the NMR Spectrometer. Square samples with an edge length of 50.0 mm and a thickness of 30.0 mm are taken. The samples are dried in a special laboratory oven. In this dry status, they are weighed and NMR-Scanned. As the small samples represent extracts from an insulated wall area, where mainly one-dimensional heat and moisture fluxes are existent, the samples are sealed at lateral and back faces with epoxy-resin. In this way, possible boundary influences as well as a run-off of condensing water can be avoided. To reduce the infiltration of the thin epoxy fluid, the sample surfaces are treated with spackle at first. All samples are stored in a climate chamber with test boundary conditions until reaching equilibrium.

TEST PROCEDURES

The tests are executed under defined boundary conditions. The test setup therefore is placed in a climate chamber with 22.5°C and 72.0% RH. The dew point temperature at these conditions is 17.2°C; the temperature generated at the surface of the carrier plate is 12.0°C. The material samples are applied to the carrier plate with heat conductive paste. All boundary conditions are measured and registered for the testing period. Regularly, the samples are removed from the test setup in order to measure moisture content and distribution. After having cleansed the samples of remaining heat conductive paste, the samples are measured gravimetrically. The samples are then brought into the NMR spectrometer one by one. A pecking motor is moving them through the inductor with 12.0 mm per step. 15 measure points are generated along each step, thus, one measuring point every 0.8 mm. While the sample is being measured in the NMR spectrometer, a slight drying is inevitable due to the existing lower relative humidity in the NMR laboratory. To account for this effect, the samples are being weight subsequently before they are put back into test setup. This procedure continues until a dynamic equilibrium is reached.

THEORETICAL CONSIDERATION

The data derived during the test should provide information about both the moisture increase over time and the amount of water gained at dynamic equilibrium. The NMR spectroscopies deliver information about the distribution of water inside the samples cross section. The measured data are dependent on the boundary conditions, as different gradients of temperature or relative humidity lead to different moisture contents and profiles in testing. Besides the material properties, the existing temperature and relative humidity of air, the temperature generated at dew point and surface temperature of the sample therefore are measured and documented. This is important for the interpretation of test results and for the identification of the material's wicking properties via numerical simulation.

Particularly the tested hydrophilic materials are expected to show a moisture gain at the beginning of the test period and subsequently a flattening of the moisture accumulation curve. Under constant boundary conditions, the initial moisture mass flow rate is dependent primarily on the vapor diffusion resistance of the material. When the relative humidity inside the material increases, the moisture accumulation curve will level off. This is due to the increasing moisture stored inside the material pores and the liquid transport back to the surface in contact with indoor air. Using the NMR-scanner, the profiles of the accumulated moisture across the material sample can be measured.

The hydrophobic mineral wool insulation, however, is used as a cross-reference. Based on its vapor diffusion permeability, a quick moisture gain at the beginning of testing is expected. Being hydrophobic, it cannot store the gained moisture at the internal pore surfaces. Therefore, no liquid transport is initiated; the condensing water is likely to stay at the cool back side of the material. As the back side of the material is sealed, the water cannot exit there. The chronological sequence of water gain therefore should not display a flattening, but a linear dependency between time and moisture gain.

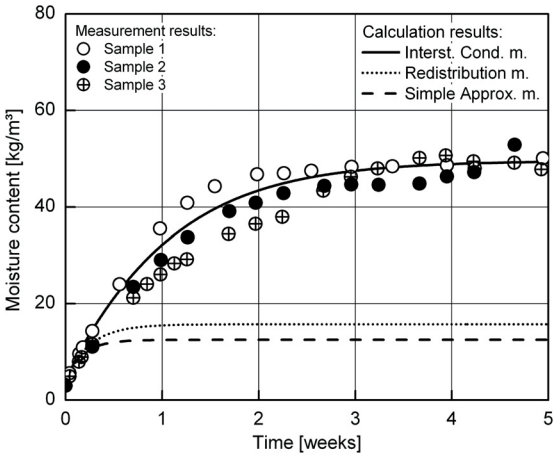

Figure 5 *Measured moisture content of calcium-silicate samples during Interstitial Condensation Test in comparison to calculated moisture gains.*

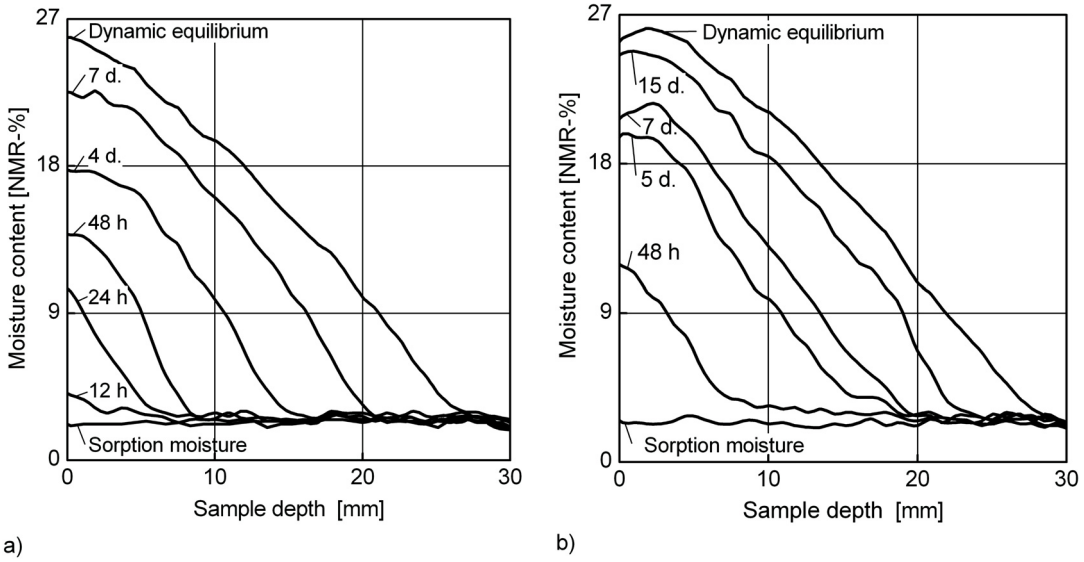

Figure 6 *Measured moisture distribution across calcium-silicate (a) sample 1 and (b) sample 2 at different points of time during Interstitial Condensation Test.*

With time advancing, more and more moisture will condense at the back side of the material. The moisture content profiles produced by the NMR should show an invariably rising amount of water at the cool back side of the material, but only sorption moisture content across the larger sections of the material.

RESULTS

Measurements

Calcium-Silicate (CS). Figure 5 shows the gravimetrically measured moisture gain of three calcium-silicate samples during the test period. Starting from a sorption moisture content of about 3.0 kg/m^3, the samples gain weight fast at the beginning of the experiment; here, measurements show a good correlation between all tested samples. With time advancing, the weight gain decreases, due to the insetting liquid transport. In this phase, measurement results display a certain discrepancy between the three samples. After approximately four weeks, a dynamic equilibrium is reached. At this point, the discrepancy between the measurement results for the different samples has declined again. The measured moisture content at dynamic equilibrium amounts to an average of approximately 49.0 kg/m^3 for all samples. The distribution of moisture across sample 1 (Figure 6a) and sample 2 (Figure 6b) shows an increase at the cool back side of the sample at the beginning of testing. Afterwards, the moisture content across the sample also rises, with its maximum remaining at the

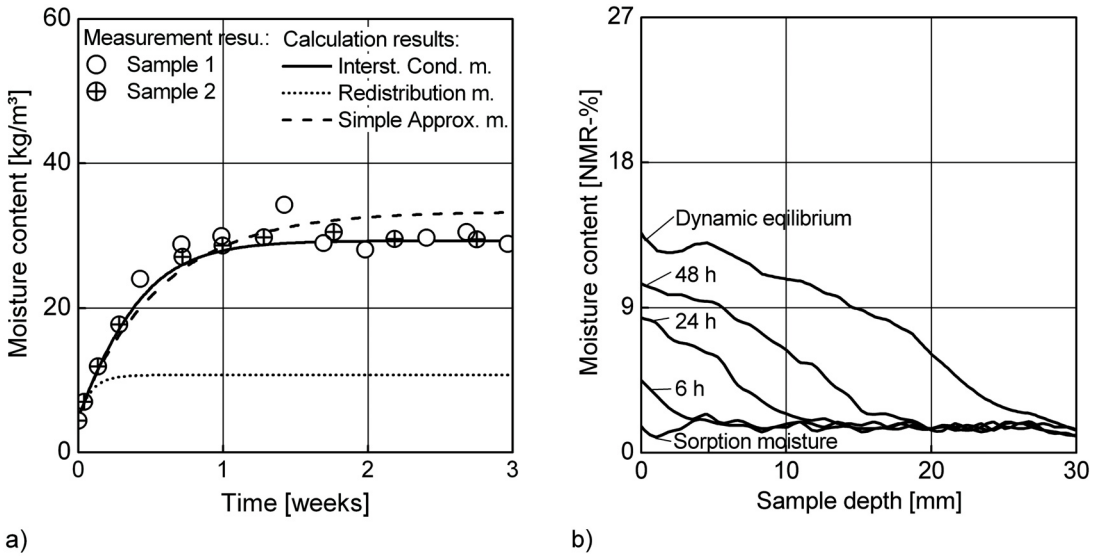

Figure 7 *(a) Measured moisture content of two AACF samples during Interstitial Condensation Test in comparison to calculated moisture gains and (b) measured moisture distribution across sample 2 during Interstitial Condensation Test.*

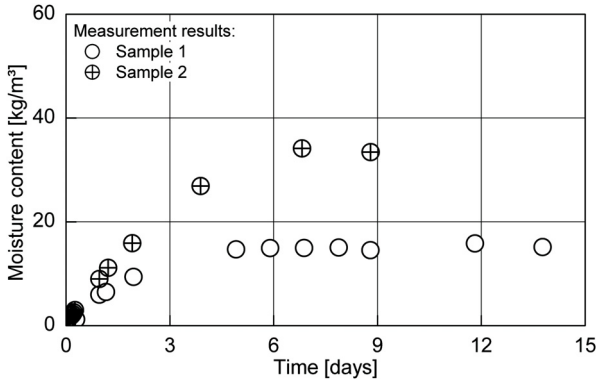

Figure 8 *Measured moisture content of two mineral wool samples during Interstitial Condensation Test.*

sealed back side and an almost linear decrease to the open-faced front surface.

Autoclaved Aerated Concrete Foam (AACF). The recorded moisture behavior of two AACF samples is shown in Figure 7a. The sorption moisture content at the beginning of testing is about 4.4 kg/m^3. The weight gain of the samples is fast at the start of the experiment and levels off with time. After approximately one week, a dynamic equilibrium is reached. The measured moisture content here is about 29.0 kg/m^3. Both samples show a good correlation of moisture gain for almost the complete test period with one exception: after approximately 1.5 weeks, a single measurement result of sample 1 shows an overshoot. The distribution of moisture across the sample (Figure 7b) shows an increase at the cooled back side of the sample at the beginning of testing. During the test period, the moisture content across the sample also increases, with its maximum remaining at the sealed back side and an even decrease to the open-faced front surface.

Mineral Wool (MW). At the beginning of experiments, a notable gain of moisture can be detected, as shown in Figure 8. Despite expectations, this gain decreases after short time. The measurement results for the two samples show a large discrepancy. For sample 1, a dynamic equilibrium seems to be reached after approximately two weeks; the moisture content here is 15.0 kg/m^3. For sample 2, however, it is reached after about seven weeks with a moisture content of 33.0 kg/m^3. The distribution of moisture across sample 1 (Figure 9a) and sample 2 (Figure 9b) differs from the profiles measured in the

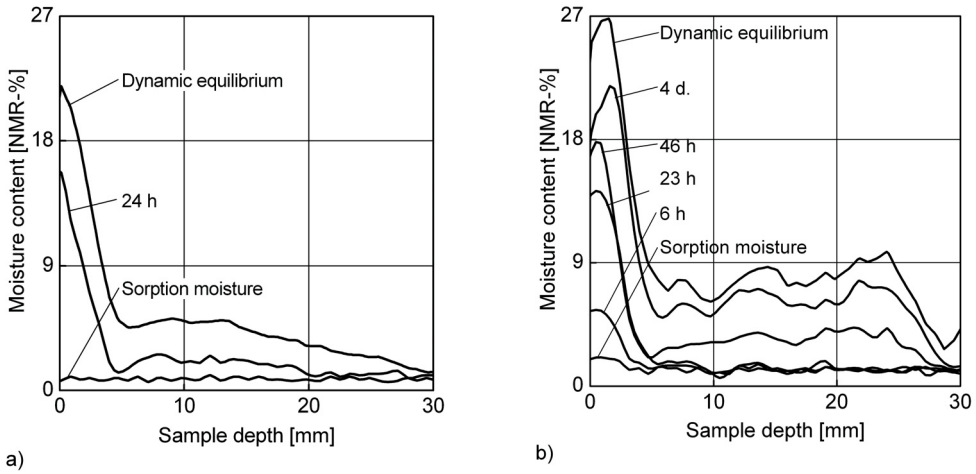

Figure 9 *Measured moisture distribution across mineral wool samples (a) 1 and (b) 2 during Interstitial Condensation Test.*

other materials. While after approximately one day already, the moisture content at the cooled back side of the material is very high, there is only little distribution of moisture across the larger part of the sample. The same behavior is shown qualitatively for all moisture distributions dynamically measured at different points of time. Since these findings do not explain why the moisture uptake of the MW sample levels off, some additional NMR scans perpendicular to the assumed 1D moisture fluxes were performed. The results show the distribution of moisture across the sample width (Figure 10a) and sample height (Figure 10b). At the lateral faces, shown to the right and left in Figure 10a, the moisture content is highest; in the bulk of the sample, a lower moisture content is recorded. Similar results are shown in the scan from top to bottom in Figure 10b, with higher values at the bottom. Both scans indicate that the condensate forming at the back side of the sample is redistributed towards the interior surface at the edges and especially at the bottom of the sample. This contradicts the assumption of a 1D moisture transport process. Moreover, it is an indication that even in hydrophobic materials the moisture may not stay at the condensation plane but move to regions where it can evaporate again. However, the small samples used in the test are certainly not representative for the situation at a real wall. Therefore the tests should be repeated with much larger samples in a kind of hot-box cold-box test. Due to the non-1D behavior of the mineral wool samples it makes no sense to do a comparative 1D hygrothermal simulation in this case.

Evaluation of New Properties via Hygrothermal Simulation

Computational simulation of the material's behavior under the test conditions. The test results for the different material samples are reproduced by numerical simulation. Here, the liquid transport coefficients derived by simple approximation are adapted step-by-step, until an acceptable correlation between calculated and measured moisture gain and distribution can be reached. The simulations are performed by using a simulation program for the intrinsic coupled heat and moisture transfer in porous building materials. Initially, the existing (measured or approximated) hygrothermal properties of the materials were employed. The resulting moisture accumulation of the calcium-silicate and the AACF samples have already been shown in Figures 5 and 7. The discrepancies between calculated and measured results are obvious and indicate an overestimation of the wicking properties; i.e. the liquid diffusivity functions at low moisture content. Therefore, the diffusivity functions D_w are lowered step by step, until a good correlation between measured data and simulation results is achieved. In this way, more realistic wicking properties can be derived. The different diffusivity functions D_w used in the simulations are shown in Figure 12. Figure 5 shows a comparison of the chronological development of both measured and calculated moisture content for calcium-silicate samples. The results for the simulation based on the new diffusivity function show a good agreement with measuring results. The results based on the function D_w determined by the Redistribution method as well as the Simple Approximation method exhibit the already mentioned discrepancies to the measuring results. In both cases, the calculated moisture content is lower than the actual moisture content; furthermore, the dynamic equilibrium is reached more quickly. The results for the moisture distribution across the samples (Figure 11a) show similar results: Acceptable agreement is obtained for the new diffusivity function, while

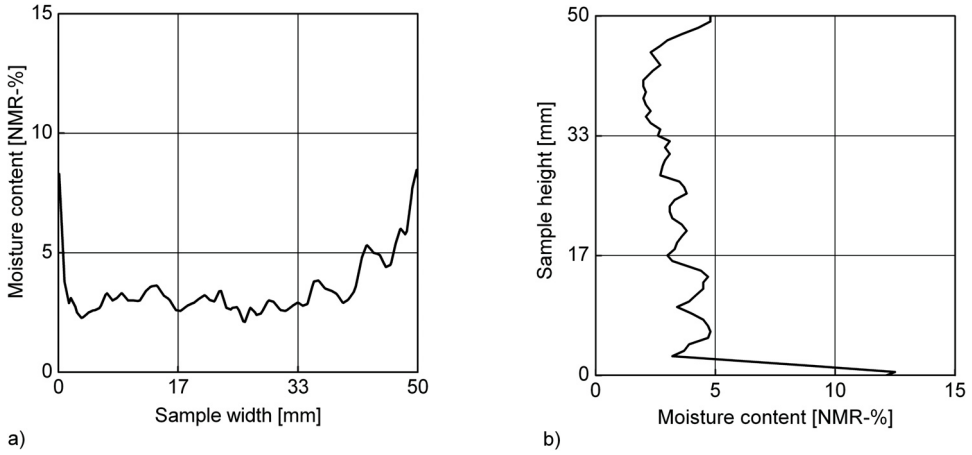

Figure 10 *Measured moisture distribution across (a) width and (b) height of mineral wool sample 1 during Interstitial Condensation Test.*

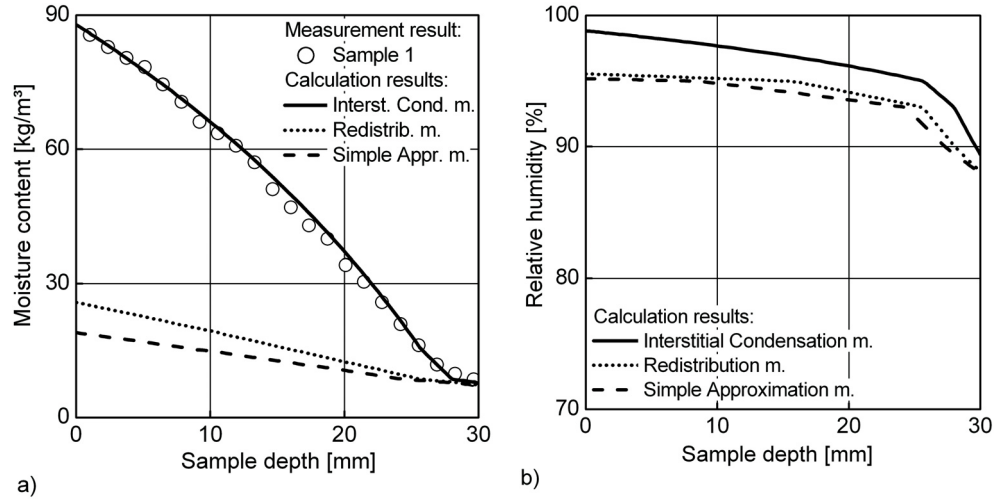

Figure 11 *Comparison of (a) measured and calculated distribution of moisture and (b) calculated relative humidity inside calcium-silicate samples during Interstitial Condensation Tests.*

the simulations with the D_w determined by the Redistribution method show large discrepancies. The relative humidity (Figure 11b) at the cool side of the insulation amounts to approximately 99% RH when the new property is used in simulations; with other properties, the highest relative humidity is approximately 95% RH.

Transfer to a real-case scenario. To further investigate the diverse results and their relevance for actual building situations, the hygrothermal behavior of a wall with calcium-silicate interior insulation is simulated in a real case scenario. The simulated solid brick wall (dimension 30.0 cm, thermal conductivity λ = 0.6 W/mK) with external mineral-based render has a thermal resistance of 0.6 m^2K/W, its heat transmission coefficient (U-factor) amounts to 1.28 W/m^2K. At the interior side of the wall, an insulation of calcium-silicate is applied. Two different board dimensions are analyzed hence. With thickness of 50.0 mm, the U-factor decreases to 0.67 W/m^2K; with 100 mm, it's reduced to 0.44 W/m^2K. All calcium-silicate properties correspond to the calcium-silicate samples used in the Interstitial Condensation Tests. The wicking properties used are the new D_w functions derived in the experiments, as well as the ones determined by the Redistribution method and the Simple Approximation method (all shown in Figure 12). For the exterior, the external climate conditions of Chicago (ORNL, cold year) are applied. The indoor climate conditions, normal moisture load, according to WTA 6-2-01 (sinusoidal variation of

indoor temperature and humidity between 20.0°C, 40% RH in winter and 22.0°C, 60.0% RH in summer), are taken as a basis for the interior. Simulation results for both insulation thicknesses display a high level of relative humidity at the boundary layer of insulation and former surface during heating period (quarters I and IV) (Figures 13a and 13b). Here, discrepancies between the results for the different liquid transport properties can be detected. In summer (quarters II and III), the construction is drying-out to a certain extent, the relative humidity therefore is lower; minor differences between different liquid transport properties are shown. It becomes obvious, too, that the discrepancies between results for the different liquid transport properties increase with rising insulation thickness. While for 50.0 mm of insulation, the difference basically is limited to the heating period, with 100.0 mm, the discrepancy in summer is also noticeable. This is due to reduced drying during summertime (quarters II and III). Figures 13c and 13d show the temperatures at the interior surface of the wall before and after thermal retrofit, as well as at the boundary layer. As expected, increasing the insulation thickness leads to an increase of the surface temperatures and to decreasing temperatures at the boundary layer during the heating period. With 50.0 mm of insulation, the temperatures at the boundary layer fall below 5.0°C, with 100.0 mm insulation thickness, temperatures below the freezing point (0°C) can be reached. In summer, the temperatures at the interior surface after thermal retrofitting fall slightly below the temperatures before thermal retrofitting. At the same time, the temperatures at the boundary layer exceed those of the interior surface. This is due to the changes in the thermal behavior of the wall after thermal retrofit. As the thermal resistance towards the interior is heightened, solar radiation increasingly contributes to a higher temperature of the wall during summer.

EVALUATION UND INTERPRETATION OF TEST AND SIMULATION RESULTS

Dew Point Experiments and Simulations

The measured results for the CS and the AACF samples show a good correlation with the initially made assumption of a quick weight gain at the beginning of testing, and an eventual flattening of weight gain. A dynamic equilibrium is reached after up to four weeks, the liquid transport back to the front is as high as the vapor transport into the material. The discrepancy shown for the weight gain of the different CS samples (Figure 5) during Interstitial Condensation Test shows the high dependency and sensitivity of the test results on the existing boundary conditions: Even slight variations in RH, air temperature and convection rates occurring during testing are reflected in slightly diverging test results.

Analyzing the results further, it becomes obvious, too, that the span of time and the amount of water gained at dynamic equilibrium cannot serve as a sole basis for predictions about the wicking ability of a material. Only the additional examination of the moisture distribution helps in revealing the actual performance of a material. In particular the results for the MW show this clearly. Against expectations, the chronological sequence of moisture gain (Figure 8) does not show a linear increase. Quite the contrary, it reaches a dynamic equilibrium faster than all other materials tested. Additionally, the amount of moisture gained at dynamic equilibrium is the lowest. Hence, it seems to show a high level of liquid back transport and capillary activity. The reasons for this behavior only become apparent when examining the moisture distribution. The characteristics shown in Figures 9 and 10 depict high amounts of moisture at the cool back of the material, as well as to the lateral faces. This leads to the assumption that once a certain level of moisture gain is

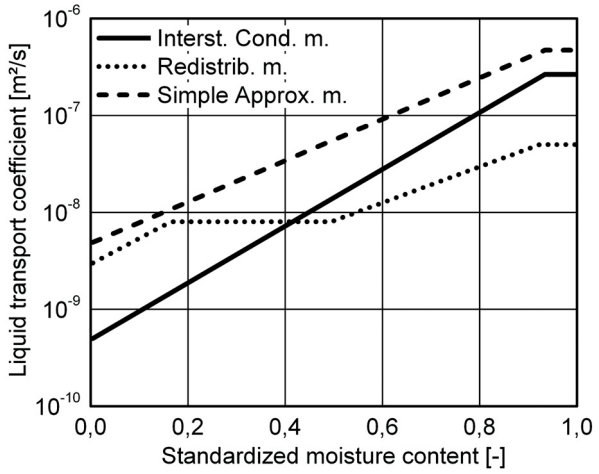

Figure 12 *Comparison of liquid transport coefficients of calcium-silicate used in the simulation. Abscissa: moisture content divided by capillary water saturation.*

reached, the existing moisture is not retained in the hydrophobic material, but is transported back to front at the lateral faces. Evidence of existing liquid moisture is exhibited by the fact that the moisture content seems highest at the bottom side of the sample (Figure 10b).

Comparisons of simulation and test results partially show discrepancies. While with the new liquid transport function, good correlations can be reached, the high deviations shown by the D_w functions detected by the Redistribution method and the Simple Approximation method may lead to underestimations of the actual moisture contents. In real construction conditions, this may lead to damage of moisture sensitive structures.

Real Case Scenario

Simulations of the real-case scenario show an increasing influence of the liquid transport coefficients with rising insulation thickness. Due to higher dew-point undercuts, higher relative humidities result beneath the insulation layer (Figures 13a and 13b). Additionally, the drying potential in summer

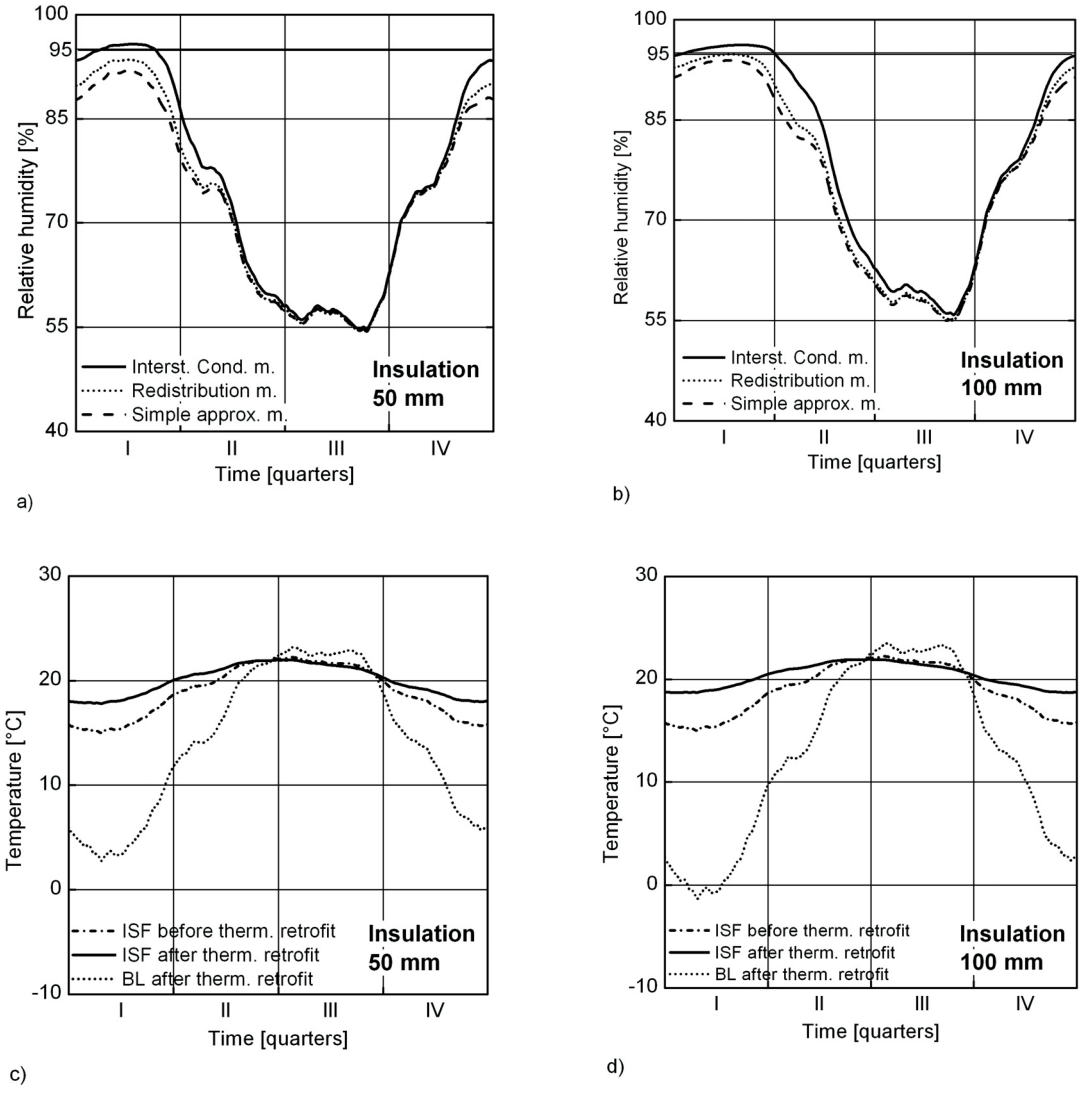

Figure 13 *Comparison of the chronological sequences of the relative humidity (monthly average values) at the boundary layer of calcium-silicate interior insulation and wall calculated with different capillary coefficients with (a) 50 mm and (b) 100 mm thickness; Chronological sequence of resulting temperature (monthly average values) at the boundary layer and interior surface with (c) 50 mm and (d) 100 mm thickness.*

decreases. While the high relative humidities detected in the dew-point tests are not displayed in the real-case scenario, the critical value of 95% relative humidity may be reached. Here, the existing 2–3% difference between simulation results with the different liquid transport properties may make the difference between functioning and failure of construction, particularly considering the reduced temperatures shown in Figures 13c and 13d. The consequence of a too positive prediction is clearly shown.

CONCLUSION

The comparison of measuring results of the Interstitial Condensation Tests and simulations based on different liquid transport properties suggests that conventionally determined D_w functions are only conditionally adequate for the performance evaluation of wicking interior insulation materials by hygrothermal simulation. Being determined at higher moisture content, these functions tend to overestimate the wicking ability of the insulation which may lead to a misjudgment of moisture gain and distribution. The detected discrepancies between the calculation results obtained with the conventional D_w functions and the D_w determined by the Interstitial Condensation Test may be significant for the performance prediction of the system. With rising insulation thickness, the discrepancies become even more pronounced. To keep the accompanying moisture damage risks for insulated constructions as low as possible, hygrothermal performance predictions have to be as accurate as possible. To assure this, and to help developing new materials with higher capillary activity in the hygroscopic region, the exact determination of a material's liquid transport ability will become more and more important in future.

REFERENCES

DIN EN ISO 12571: Bestimmung der hygroskopischen Sorptionseigenschaften, April 2000

DIN EN ISO 12572: Bestimmung der Wasserdampfdurchlässigkeit, September 2001

DIN EN ISO 15148: Bestimmung des Wasseraufnahmekoeffizienten bei teilweisem Eintauchen, März 2003

Holm, A., Krus, M.: Bestimmung des Transportkoeffizienten für die Weiterverteilung aus einfachen Trocknungsversuchen und rechnerischer Anpassung, in: Bauinstandsetzen 4, 1998, H. 1, S. 33-52

Krus, M.: Feuchtetransport- und Speicherkoeffizienten poröser mineralischer Baustoffe. Theoretische Grundlagen und neue Messtechniken, Dissertation Universität Stuttgart, 1995

Künzel, H.M.: Verfahren zur ein- und zweidimensionalen Berechnung des gekoppelten Wärme- und Feuchtetransports in Bauteilen mit einfachen Kennwerten, Dissertation Lehrstuhl Bauphysik, Fakultät Bauingenieur- und Vermessungswesen der Universität Stuttgart, 1994

Krus, M., Holm, A., Schmidt, Th: Ermittlung der Kapillartransportkoeffizienten mineralischer Baustoffe aus dem w-Wert, Internationale Zeitschrift für Bauinstandsetzen 3, 1997, H. 3, S. 1-16

Scheffler, G., Plagge, R.: Ein Trocknungskoeffizient für Baustoffe, in: Bauphysik, 2009 Nu. 31, S. 125-138

WTA Merkblatt 6-2-01/D